Journal of Nuclear Materials 421 (2012) 97–103

Contents lists available at SciVerse ScienceDirect

Journal of Nuclear Materials

journal homepage: www.elsevier.com/locate/jnucmat

Study of PRIMAVERA steel samples by positron annihilation spectroscopy technique II – Lifetime measurements

V. Krsjak [a,*], V. Grafutin [b], O. Ilyukhina [b], R. Burcl [a], A. Ballesteros [a], P. Hähner [a]

[a] European Commission, Joint Research Centre, Institute for Energy and Transport, P.O. Box 2, 1755 ZG Petten, Netherlands
[b] Institute of Theoretical and Experimental Physics, B. Cheremushkinskaya 25, 117218 Moscow, Russia

ARTICLE INFO

Article history:
Received 30 September 2011
Accepted 25 November 2011
Available online 3 December 2011

ABSTRACT

In the present article, a positron annihilation lifetime technique was used for the study of VVER-440/230 weld materials, manufactured in the frame of the international PRIMAVERA project on microstructural investigation of the irradiated WWER-440 reactor pressure vessel steel. The present results complement our previous report of positron angular correlation experiments and provide in-depth characterization of vacancy type defects behavior under irradiation and thermal treatment. The results give new insight into the previously published atom probe tomography and angular correlation of annihilation radiation studies. The measurements do not show any association of phosphorus or its segregation to the open volume defects investigated by positron annihilation spectroscopy. The embrittlement effects related to the phosphorus seem to be effectively annealed-out during 475 °C thermal treatment and the post annealing microstructure and mechanical properties of the material are consequently affected mostly by agglomerations of vacancy clusters coarsened during thermal treatment.

1. Introduction

The phenomenon of radiation embrittlement has been well described in the last decades for both Western and Eastern materials used in nuclear reactors. A number of experimental works has provided data, which can be used in the prediction of the behavior of current generation reactor pressure vessel (RPV) materials beyond the end-of-lifetime fluence [1–3]. The role of the various alloying elements has been studied along the fabrication of hundreds of model alloys. In order to improve the understanding of various microstructural processes, many advanced analytical techniques have been involved in the study of radiation effects [3–6]. Application of these techniques in the study of irradiated nuclear materials requires not only the knowledge of the role of individual parameters like chemical composition, neutron flux, fluence, irradiation temperature, but also their complex interactions.

One of the key issues in the extension of the operation of the Russian type VVER nuclear reactors is the thermal annealing of the RPV. Phosphorus segregation and cooper enriched precipitates were found to be the critical factors in the radiation embrittlement, but their effect on the result of annealing recovery is not fully understood yet. The international project PRIMAVERA was established in order to extend the current knowledge and to predict the behavior of VVER RPV after post-annealing re-irradiation. Various experimental techniques have already been applied to the study of model materials with various phosphorus contents. The results of tensile tests, Charpy impact tests and tomographic atom probe investigations have been published recently [7,8]. Two different techniques based on positron annihilation spectroscopy (PAS) were included in the PRIMAVERA test matrix. The results of angular correlation of annihilation radiation (ACAR) have been reported in our previous paper [9]. In the present study, we discuss the results of a second PAS technique – lifetime measurements. While the ACAR results provided mostly the information about electronic environment around the annihilation sites, positron annihilation lifetime spectroscopy (PALS) allows one to distinguish whether annihilation occurs in defect-free bulk or in various types of lattice defects.

2. Experiment

The weld 501, produced in accordance to standard technology for the first generation of VVER-440 has been used in this project [8]. In the radial direction of this weld, a typical gradient of the phosphorus content was observed. Consequently, three different groups of samples with phosphorus content varying in the range 0.025–0.040 wt.% were prepared. These samples, designated as LP, MP and HP (low, medium and high phosphorus) were investigated in the (i) unirradiated, (ii) irradiated (two different neutron fluence levels) and (iii) irradiated and annealed state. Phosphorus content (which is considered to be one of critical parameters for radiation embrittlement of the Russian reactor steels) and chemical composition of the samples are given in Table 1. It is important to note the

* Corresponding author.
E-mail address: vladimir.krsjak@ec.europa.eu (V. Krsjak).

0022-3115/$ - see front matter © 2011 Elsevier B.V. All rights reserved.
doi:10.1016/j.jnucmat.2011.11.067

Table 1
Chemical composition (in wt.%) of the investigated PRIMAVERA steel samples with low, medium and high (LP, MP, HP) phosphorus content, conventional VVER-440 base 15Kh2MFA (BM) and weld Sv-10KhFMT (WM) material (Fe balance).

Material	C	Si	Mn	**P**	S	Cr	Ni	Mo	Cu	V
LP	0.04	0.04	1.12	**0.027**	0.013	1.42	0.13	0.49	0.16	0.19
MP	0.04	0.39	1.15	**0.031**	0.013	1.42	0.13	0.50	0.16	0.18
HP	0.05	0.36	1.09	**0.038**	0.014	1.54	0.13	0.51	0.16	0.19
WM	0.04	0.59	1.1	**0.012**	0.017	1.37	-	0.50	0.06	0.20
BM	0.16	0.17	0.46	**0.014**	0.016	2.9	0.07	0.66	0.07	0.31

higher phosphorus and copper content, as compared to conventional VVER-440 weld (Sv-10KhFMT, WM) and base (15Kh2MFA, BM) material.

Although the direct sensitivity of the PALS technique to the segregation of P and precipitation of Cu is limited when the content of these elements is low [10], it is known that these processes may produce new sinks for radiation induced defects and affect the nucleation of large open volume defects [11], which can be probed by PALS.

Irradiation of the PRIMAVERA materials has been performed by Russian Research Centre, Kurchatov Institute (RRC KI). Bulk samples were irradiated to two different doses at 270 °C. Irradiations to a lower fluence ($\sim 1.2 \times 10^{23}$ m^{-2}) were performed with a neutron flux of 0.4×10^{16} m^{-2} s^{-1} in the surveillance channels of Rovno1 NPP (Ukraine). Irradiations to a higher fluence ($\sim 6 \times 10^{23}$ m^{-2}) were performed with a neutron flux of 2×10^{16} m^{-2} s^{-1} in the surveillance channels of Rovno2 NPP. Individual neutron fluences are listed in Table 2. After irradiation to a fluence of $\sim 6 \times 10^{23}$ m^{-2}, one set of samples was annealed using the standard annealing procedure for VVER-440 RPV (475 °C/100 h).

Positron lifetime measurements of the PRIMAVERA materials were performed at Institute of Theoretical and Experimental Physics, Russia. The experimental equipment was based on fast BaF_2 scintillators coupled with XP1020 photomultipliers. Discrimination of the signals was achieved by Ortec 583B discriminators in a coincidence configuration (Ortec 414A) and the final lifetime spectra were stored in a PC equipped with multi-channel analyzer card.

The positron source used in the experiments was prepared by evaporation of aqueous solution of ^{22}NaCl (Na isotope 22) with volume activity 37 MBq/ml. Two 7.5 μm polymer foils (Lavsan) were used for the encapsulation of the positron source according the ISO 2919 standard. The activity of the positron source was determined to be 2.95 MBq, using a ^{44}Ti calibration source with known activity.[1]

It was reported earlier that conventional lifetime measurements of irradiated materials containing ^{60}Co with use of ^{22}Na positron cannot be performed straightforward [12]. Three detector coincidence setup described in the paper of Cizek et al. can effectively discriminate the spurious ^{60}Co signals, since only triple coincidences belonging to ^{22}Na (1274 keV start photon plus two annihilation photons 511 keV) are accepted for the lifetime spectrum. Our approach, however, is based on the conventional two detectors setup exploited in a series of complementary measurements with various combinations of irradiated sample – unirradiated sample – positron source, in order to precisely determine the effect of ^{60}Co on the lifetime spectrum. Our measurements have shown that when the activity of the ^{60}Co is sufficiently lower than the ^{22}Na activity (~25% for high irradiated materials, see Table 2), ^{60}Co contributions to the lifetime spectra can be determined and properly taken into account in the spectra evaluation. The first contribution is an increase of the background due to ^{22}Na–60Co coincidences. As can be seen in Table 2, this contribution makes up to 42% of the background value for high irradiated materials and 13–18% for the low irradiated materials. The second contribution, measured on irradiated samples without ^{22}Na source, characterizes the contribution of ^{60}Co prompt peak to the signal. It was determined to contribute up to 9.3% of the signal counts for high irradiated materials and ~2% for the low irradiated materials. As this component is identical to a zero lifetime, it was fixed in the fitting program as narrow Gaussian (e.g. 0.1 ps) shifted by 80–100 ps to the left from the lifetime peak. The contribution of this component to the background was estimated to be less than 2% for high irradiated materials and therefore it was neglected.

The approach described above can be summarized by the following steps (scheme A–B–Na(X)–B–A describe the source sandwich setup, where A is the outer sample, B is the inner sample and Na (X) is the positron source or source dummy respectively).

2.1. Measurement of non-irradiated sample and determination of source contribution

- Measurement of pure material with known lifetime (Si monocrystal) Si–Na–Si.
- Determination of the free parameters (all intensities and one largest component lifetime) by fixing the lifetimes of Si and Lavsan.
- Measurement of the non-irradiated material tiled by material equivalent dummy sample (DS) to keep the geometry of consecutive measurements of irradiated samples DS-LP1-Na-LP1-DS.
- Determination of positron lifetimes and intensities of the measured sample by fixing the positron source components.

2.2. Measurement of irradiated sample and determination of Co^{60} effect (LP2 sample)

- Determination of Na–Co effect on background by measurement in LP2-LP1-Na-LP1-LP2 setup and following subtraction of DS-LP1-Na-LP1-DS spectrum background.
- Determination of prompt Co peak by measurement of LP1 -LP2-X-LP2-LP1.
- Measurement of irradiated sample (LP1-LP2-Na-LP2-LP1).
- Determination of positron lifetimes and intensities of the measured sample by fixing the positron source components, prompt Co^{60} peak and background.

The same procedure was carried out for the LP3,4, MP2-4 and HP2-4 samples.

When we consider two distinct types of defects in the bulk material, individual trapping rates can be described as

$$\kappa_{d1} = \frac{I_2}{I_1}[I_3(\lambda_{d1} - \lambda_{d2}) + (\lambda_b - \lambda_{d1})], \quad (1)$$

$$\kappa_{d2} = \frac{I_3}{I_1}[I_2(\lambda_{d2} - \lambda_{d1}) + (\lambda_b - \lambda_{d2})], \quad (2)$$

[1] The energy of gamma quanta from ^{44}Ti (1.16 MeV) is comparable to the gamma energy from ^{22}Na (1.28 MeV) and therefore the count rate ratio is equal to the ratio of activities of these sources.

Table 2
Neutron fluences, relative ^{60}Co activities and individual cobalt contribution to the experimental spectra – calculated for each pair of samples (annealed samples are designated by asterisk).

Sample	Fluence ($E > 0.5$ MeV) (m^{-2})	^{60}Co activity – relative to ^{22}Na (%)/volume activity (MBq/g)	^{60}Co peak contribution to lifetime spectrum (%)	^{60}Co contribution to signal background (%)
LP1	0	–	–	–
LP2	1.13×10^{23}	7.6/0.26	2.1	18.0
LP3	5.31×10^{23}	26.6/1.59	9.3	42.0
LP4	$5.66 \times 10^{23*}$	24.2/1.54	7.7	40.6
MP1	0	–	–	–
MP2	1.24×10^{23}	4.8/0.50	2.0	15.5
MP3	6.39×10^{23}	22.9/1.68	7.6	36.4
MP4	$5.94 \times 10^{23*}$	20.0/1.53	6.6	36.4
HP1	0	–	–	–
HP2	1.22×10^{23}	5.3/0.46	2.0	13.0
HP3	5.95×10^{23}	22.8/1.81	7.7	38.0
HP4	$5.71 \times 10^{23*}$	24.1/1.68	8.3	38.4

where $\lambda_b = \frac{1}{\tau_b} + \kappa_{d1} + \kappa_{d2}$; $\lambda_{d1} = \frac{1}{\tau_2}$; $\lambda_{d2} = \frac{1}{\tau_3}$ are the annihilation rates in bulk, defect 1 and defect 2, respectively and I_1, I_2 and I_3 are the intensities of individual components.

For a given type of defects, the positron trapping rate κ_d is proportional to the defect concentration C_d:

$$\kappa_d = C_d \mu_d, \tag{3}$$

Here μ_d is the positron trapping coefficient for the particular defect type. For small vacancy clusters ($n < 10$) positron trapping rate is proportional to the number of vacancies in the cluster and the concentration of small clusters can be written as

$$C_{nV} = \frac{\kappa_{VC}}{n\mu_{1V}}, \tag{4}$$

where μ_{1V} is positron trapping coefficient for mono-vacancies. In case of spatially extended defects, such as voids or precipitates, positron mobility (diffusion to the defects) starts to limit the total trapping rate [13]. Here, the diffusion limited trapping provides more reliable results and positron trapping rate is given by:

$$C_{VC} = \frac{\kappa_{VC}}{4\pi r_{eff} D_+}, \tag{5}$$

where $D_+ = (1 \pm 0.5) \times 10^{-4}\ m^2\ s^{-1}$ [14] is the positron diffusion constant for Fe at 300 K, and r_{eff} denotes the effective radius of the extended defects.

3. Results and discussion

After subtracting the background and fixing the ^{60}Co prompt contribution, the corrected spectra were fitted in the LT9.0 program [15]. The source contribution with total intensity of 30% was fixed as 175 ps, 427 ps and 1.84 ns components, which corresponds to annihilation in NaCl and Lavsan foil. Two Gaussians with fixed intensity 0.85 and 0.15 (FWHM ~300 ps or ~600 ps respectively) were used to describe the resolution function affecting all measured lifetime spectra. The contribution of prompt ^{60}Co peak was fixed as very narrow component (~0.1 ps), the intensity of which was found to be in very good agreement with calculated contributions listed in Table 2.

In all studied samples positron lifetime components of 120 ps and 255 ps were found. These components correspond to annihilation in the bulk (and dislocations) and annihilation in small clusters of 4–5 vacancies [16]. In addition, a large component (350 ps) found in the irradiated materials was attributed to large vacancy clusters ($r \sim 4$ Å) [9]. All lifetime components were fixed, leaving the intensities as free parameters to be determined. Qualitative changes in vacancy type defects were consequently characterized as relative changes of the intensities of the individual components. The obtained results are listed in Table 3.

In the materials with low and medium phosphorus content, an increase of the bulk component as well as a decrease of positron mean lifetime (MLT) after the first level of irradiation was observed (Fig. 1). This can be attributed to the thermal annealing effect due to irradiation temperature enhanced by thermal spikes from displacement cascades, which is a competitive process to radiation induced defect formation. The origin of this effect was described by Brauer et al. as changes in the shape of carbides accompanied by a decrease of the effective number of vacancy-like misfit defects [17]. As a result of that annealing, we observed that positron trapping at vacancy type defects decreases after irradiation to $\sim 1.2 \times 10^{23}\ m^{-2}$ at 270 °C (Fig. 2a and b). Similar behavior was observed by Slugen et al. [3] who reported decreasing positron lifetimes after irradiation up to $7.8 \times 10^{23}\ m^{-2}$ at 285–298 °C. It must be stressed, however, that the irradiation reported in that paper was performed with slightly higher neutron flux than the present PRIMAVERA irradiations (factor 5). It is known that higher fluxes promote dynamic recovery leading to less pronounced radiation damage (e.g. swelling) in reactor steels [18]. We assume that this is the reason that in the present paper no decreasing of any positron lifetime component was observed at fluence above $5 \times 10^{23}\ m^{-2}$.

As can be seen in Fig. 1, the highest positron trapping at defects and the highest positron mean lifetime in the non-irradiated material was observed for the lowest phosphorus content (LP). This indicates the highest concentration of various microstructural defects (lattice imperfections) which can act as a positron traps. This assumption is supported also by the previously performed mechanical tests which show the LP material to have the highest yield strength as well as highest ductile to brittle transition temperature [19]. Both properties, hardness and brittleness, can be associated to the presence of lattice imperfections predicted by PAS. Comparison of the positron mean lifetime MLT and the yield strength ($Rp_{0.2}$) for the nonirradiated materials can be seen in the Table 4.

According to Eqs. (1)–(5) positron trapping rates and concentration of both assumed types of defects were obtained (Table 5). The concentration of small defects is rather constant throughout the experiment with notable decrease after thermal annealing. This points out that the creation of vacancies induced by radiation is accompanied by the coarsening of these defects due to radiation and thermal aging. At a certain fluence ($\sim 5 \times 10^{23}\ m^{-2}$) the agglomeration of vacancies can collapse into dislocation loops [5,20], which can be observed as an unexpected change of the trend of positron lifetime parameters. As can be seen in Fig. 3a and b, such behavior was observed for the large vacancy cluster component of LP and MP materials. One of possible interpretation can be indeed the collapsing of vacancy clusters ($\tau \sim 350$ ps) into dislocation loops ($\tau \sim 150$ ps). Another reason however, can be the different rate of radiation damage accumulation, since the lower fluence was obtained with a neutron flux of $0.4 \times 10^{16}\ m^{-2}\ s^{-1}$, while the higher

fluence was obtained with a neutron flux 2×10^{16} m^{-2} s^{-1}. As mentioned above, lower neutron fluxes lead to more pronounced radiation damage and therefore to qualitatively and quantitatively more damage.

The general effect of annealing on the irradiated materials can be seen in Fig. 1 and Fig. 3a–c. In all three materials, the 475 °C annealing led to an increase of the bulk component, which means reduction of positron trapping at defects. When, however, two defect types are considered, distinct behaviors can be observed. While the concentration of small VC decreases, the positron trapping at large clusters/voids increases after annealing. This can be generally attributed to the thermal coarsening of the vacancy clusters. According to the previous ACAR experiments [9], these clusters can be characterized as voids surrounded by Fe ions as no decoration of these voids by impurity atoms was found. This points out that the accumulation of the radiation induced point defects and post irradiation coarsening of these defects is not predominantly localized in the precipitates although their role on the precipitation mechanism is still to be determined.

Coarsening of vacancy clusters similar to that described above was reported by Bergner et al. for Cu-enriched VVER-type model alloys after annealing at 475 °C for 100 h [21]. In the same work, however, this effect was not observed in low-Cu alloy, where during the annealing process dissolution of these defects preferably takes place. Accordingly, Slugen et al. [22] reported significant annealing of small as well as large vacancy type defects in low-P, low-Cu VVER alloys. Tomographic atom probe study performed on PRIMAVERA materials [7] confirmed large Cu-rich precipitates after post-annealing re-irradiation. Coarsening of these nano-features or changes in the shape of precipitate/matrix interface are potential candidates for void nucleation site [17], but further studies are needed to confirm this.

The correlation of the present results with earlier investigations of the mechanical properties [7] is unfortunately not completely straightforward and must be discussed with respect to different mechanism taking place in the microstructure of the irradiated materials. Only the processes affecting both mechanical properties of the material and positron trapping kinetics can be discussed in common terms. However, there are processes significantly affecting the mechanical properties of the material under irradiation (e.g. segregation and precipitation), but they have only little (direct) effect on positron trapping (although they might be still studied by PAS in a simple model materials).

Let us assume that the thermal annealing of the irradiated materials has led to a significant annihilation of radiation induced precipitates (features that PAS is here not sensitive to) and similar vanishing of dislocation loops [23]. Here the transition from the non-irradiated state to irradiated and annealed state, on the level of vacancy agglomerates, becomes an important factor in the aging of material microstructure. When the process of thermal aging induces both, annealing of small vacancy type defects and coarsening of large vacancy agglomerates, positron mean lifetime values do not necessarily characterize the difference between non-irradiated material and irradiated and annealed material. Here, more reliable results can be obtained from the lifetime components describing just the large defects. These defects, if present in the material, play an important role in the evolution of physical and mechanical properties. Table 6 contains a comparison of yield strength ($Rp_{0.2}$), ductile–brittle transition temperature (DBTT) and intensity of VC components from PALS measurements (I_3) for the three materials studied. We assume that the presence of large open volume defects increases the strength and decreases the ductility of the irradiated and thermally aged material in comparison to the initial non-irradiated state. Without the thermal annealing, mechanical properties of the irradiated material are then given by a combination of several factors (formation of dislocation loops, precipitation, segregation, vacancy agglomeration, etc.). It seems that the vacancy agglomerates play only a minor role here so that positron annihilation cannot provide a clear information on the radiation embrittlement.

Table 3
Intensities of the positron lifetime parameter in the studied materials.

Material	I_1 (%)	I_2 (%)	I_3 (%)	Fit's variance	Backgr.	MLT (ps)
LP1	56.5	43.5	0	0.97	47.5	178.7
LP2	67.4	25.2	7.4	1.36	134.7	171.0
LP3	60.1	35.3	4.7	1.08	169.2	178.6
LP4	67.4	24.4	8.2	0.92	167.7	171.7
MP1	59.0	41.0	0.0	1.00	106.3	175.3
MP2	63.4	32.6	4.0	1.01	124.8	173.1
MP3	58.8	41.1	0.1	1.10	173.4	175.8
MP4	61.3	34.2	4.5	0.83	164.6	176.5
HP1	59.4	40.7	0	1.06	102.2	174.9
HP2	58.8	41.2	0	0.93	117.1	175.6
HP3	59.2	37.6	3.3	0.89	163.0	178.2
HP4	64.0	28.8	7.2	1.03	164.6	175.3

4. Conclusions

The positron annihilation lifetime experiments reported in the present paper were conducted as part of the PRIMAVERA programme on microstructural investigation of the irradiated WWER-440 reactor pressure vessel steel. The obtained results complement previous ACAR experiments on irradiated (and subsequently annealed) VVER model materials. Although both techniques are based on the electron–positron interaction, each technique provides different types of information about microstructural changes induced by radiation and thermal treatment.

New experimental and data processing procedures were proposed to overcome the high radiation background of ^{60}Co, which significantly disturbs the positron lifetime experiments when a conventional ^{22}Na positron source is used. The present procedure employs standard two detector coincidence setup of the spectrometer instead of three detector coincidence setup, usually applied for the elimination of ^{60}Co prompt peak. The main advantage of this approach is the avoidance of a significant reduction in count-rate, necessarily linked with the three detector setup.

Our experiments showed that basically three different processes play a role in the microstructure evolution. All processes, irradiation induced creation of point defects, thermally induced annealing of these defects and thermal/irradiation induced coarsening of defects were considered in the interpretation of results. As can be seen in the positron mean lifetime values, thermal annealing of small defects is the dominant effect in the first level of irradiation of steels with low and medium phosphorus content. The material with the high P content showed only negligible changes in the PALS parameters after irradiation to neutron fluence of 1.2×10^{23} m^{-2}. This material was also resistant to agglomeration of large voids, which have been observed in LP and MP materials already at first fluence level. Creation of radiation induced defects was observed in all studied materials irradiated to fluence $\sim 6 \times 10^{23}$ m^{-2} as an increase of positron mean lifetime. The most pronounced increase (7.8 ps) was found in LP material. This however cannot be directly linked with the radiation embrittlement without considering the well known effects of phosphorus segregation and copper precipitation. Although these processes may be investigated by PAS in some defect-free model materials, they can be hardly distinguished in the PALS spectra of real materials containing additional types of lattice imperfections acting as positron traps. Nevertheless, the correlation of the present results with the previous mechanical tests is reasonable in certain cases.

As our measurements showed, the role of the vacancy type defects, though hardly distinguishable during irradiation, can be

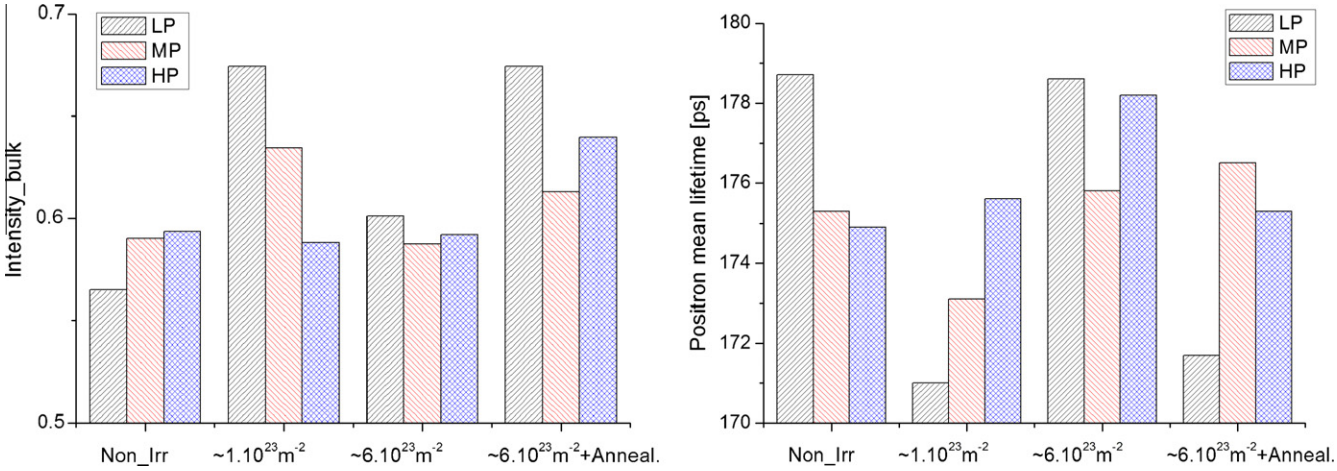

Fig. 1. Intensity of positron lifetime in defect-free bulk (left) and positron mean lifetime (right).

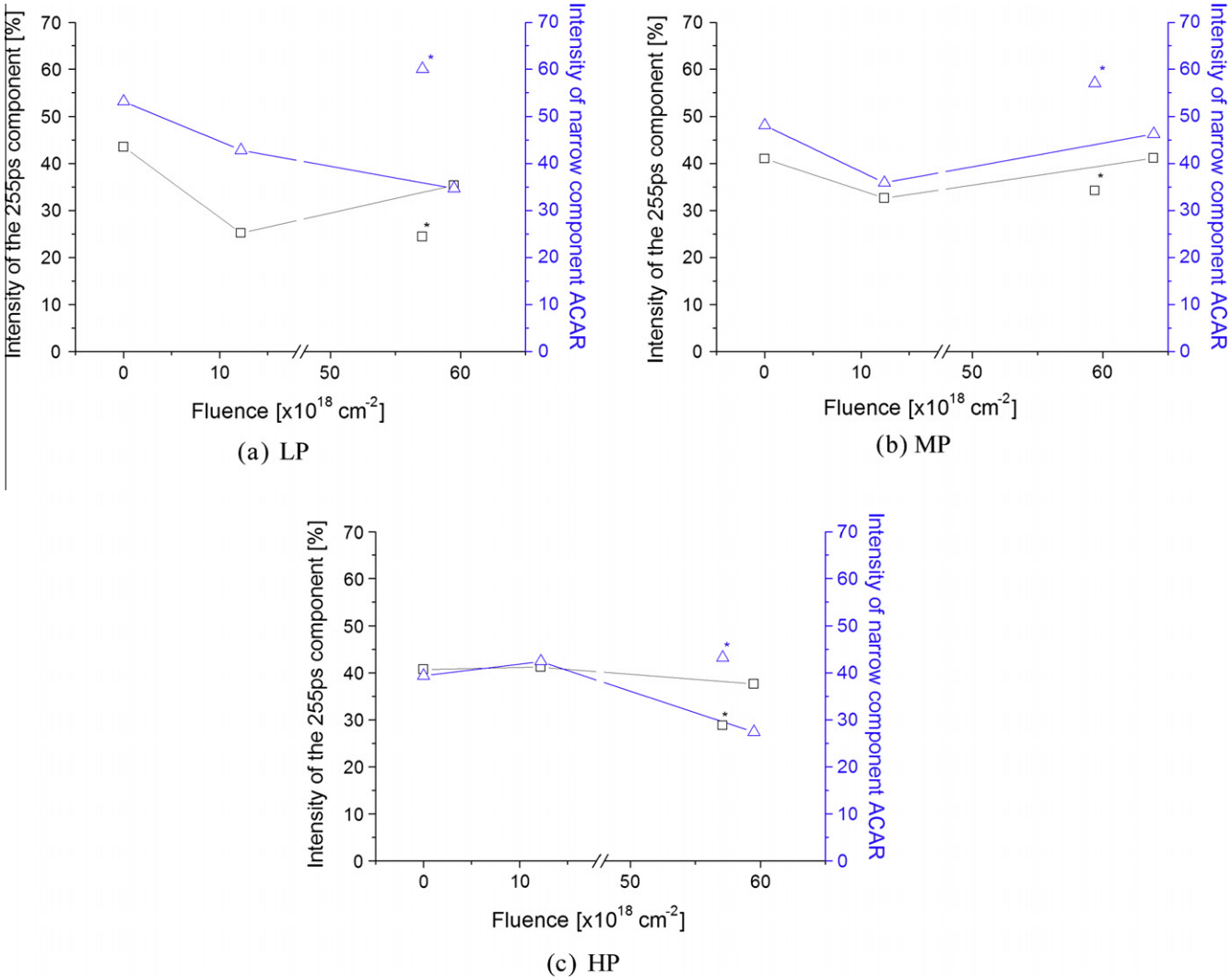

Fig. 2. Intensities of small (point) defects component from positron lifetime measurements (□) and narrow Gaussian component from ACAR measurements characterizing open volume defects (△) published in [9].

investigated in the annealed microstructure. The microstructure properties after recovery annealing (dissolution of the radiation induced precipitates and annealing of dislocations) is more sensitive to the behavior of vacancy type defects and particularly to their

Table 4
PALS and tensile test results of the non-irradiated materials.

Material	MLT (ps)	$Rp_{0.2}$ (MPa)
LP1	178.7	534
MP1	175.3	505
HP1	174.9	492

Table 5
Positron trapping rates and concentrations derived from the experimental data for small vacancy clusters (4 V) and large vacancy clusters (VC).

Material	κ_1 (s^{-1})	κ_2 (s^{-1})	$C_{(V3)}$ (m^{-3})	$C_{(VC)}$ (m^{-3})
LP1	3.86×10^9	0	9.89×10^{22}	0
LP2	1.90×10^9	6.37×10^8	4.87×10^{22}	1.27×10^{21}
LP3	2.97×10^9	4.48×10^8	7.61×10^{22}	8.92×10^{20}
LP4	1.84×10^9	7.04×10^8	4.72×10^{22}	1.40×10^{21}
MP1	3.48×10^9	0	8.92×10^{22}	0
MP2	2.59×10^9	3.59×10^8	6.65×10^{22}	7.14×10^{20}
MP3	3.51×10^9	1.05×10^7	8.99×10^{22}	2.10×10^{19}
MP4	2.82×10^9	4.20×10^8	7.23×10^{22}	8.35×10^{20}
HP1	3.43×10^9	0	8.80×10^{22}	0
HP2	3.51×10^9	0	8.99×10^{22}	0
HP3	3.20×10^9	3.12×10^8	8.21×10^{22}	6.21×10^{20}
HP4	2.29×10^9	6.48×10^8	5.86×10^{22}	1.29×10^{21}

Table 6
PALS, tensile test and impact test parameters of the irradiated and annealed materials.

Material	I_3 (%)	$Rp_{0.2}$ (MPa)	DBTT (°C)
LP4	8.2	558	47
MP4	4.5	524	23
HP4	7.2	558	26

agglomeration. This, as we assume, can be linked with the results of Charpy and tensile tests and therefore with the mechanical properties. Having this in mind, we can consider the annealing process to be most effective for the material with medium (0.031 wt.%) phosphorus content. We assume that the better ductility found in this material is enhanced by a low concentration of large open volume defects. These were found in all annealed materials with positron lifetime spectroscopy as well as angular correlation measurements. Although the ACAR technique did not show any connection between vacancy accumulation and precipitation/segregation of the impurities (copper, phosphorus), the role of vacancies on these processes is still not understood and must be further studied.

The present paper together with published reports show that the PAS techniques represent complementary tools for microstructural investigation. A combination of positron lifetime technique with techniques based on momentum distribution of annihilation radiation (ACAR or eventually the Doppler broadening spectroscopy) can provide unique information about size and distribution of the vacancy type defects.

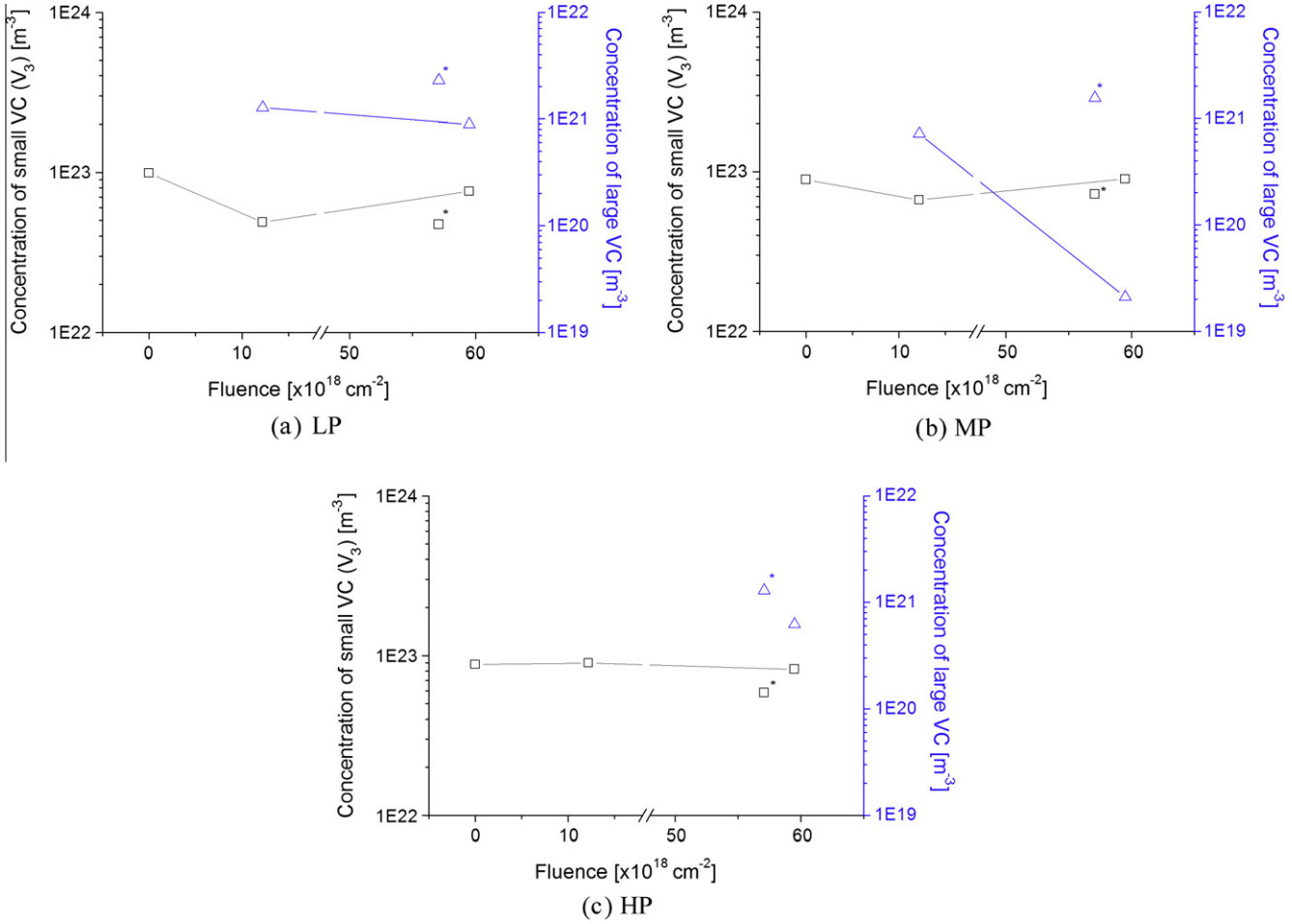

Fig. 3. The concentrations of two observed types of defects (□ – small cluster of three vacancies; △ – large vacancy cluster) calculated from the PALS results.

References

[1] M.K. Miller, A.A. Chernobaeva, Y.I. Shtrombakh, K.F. Russell, R.K. Nanstad, D.Y. Erak, O.O. Zabusov, J. Nucl. Mater. 385 (2009) 615–622.
[2] M. Valo, L. Debarberis, A. Kryukov, A. Chernobaeva, Int. J. Pres. Vess. Pip. 85 (2008) 575–579.
[3] V. Slugen, J. Kuriplach, P. Ballo, P. Domonkos, G. Kögel, P. Sperr, W. Egger, J. Nucl. Mater. 302 (2002) 89–95.
[4] B. Acosta et al., Nucl. Eng. Des. 235 (2005) 1951–1959.
[5] J. Kocik, E. Keilova, J. Cizek, I. Prochazka, J. Nucl. Mater. 303 (2002) 52–64.
[6] S.E. Cumblidge, A.T. Motta, G.L. Catchen, G. Brauer, J. Böhmert, J. Nucl. Mater. 320 (2003) 245–257.
[7] S. Rogozkin, A. Chernobaeva, A. Aleev, A. Nikitin, A. Zaluzhnyi, D. Erak, Ya. Shtrombakh, O. Zabusov, L. Debarberis, A. Zeman, The effect of post-irradiation annealing on VVER-440 RPV materials mechanical properties and nano-structure under re-irradiation, in: Proceedings of PVP2009, 2009 ASME Pressure Vessels and Piping Division Conference, July 26–30, 2009, Prague, Czech Republic, PVP2009-78128.
[8] A. Chernobaeva, Y. Shtrombah, A. Krjukov, D. Erak, P. Platonov, J. Nikolaev, E. Krasikov, L. Debarberis, Yu. Kohopaa, M. Valo, Vodenicharov, Int. J. Pres. Vess. Pip. 84 (2007) 151–158.
[9] V. Grafutin, O. Ilyukhina, V. Krsjak, R. Burcl, P. Hähner, D. Erak, A. Zeman, J. Nucl. Mater. 406 (2010) 257–262.
[10] A. Zeman, L. Debarberis, L. Kupca, B. Acosta, M. Kytka, J. Degmova, J. Nucl. Mater. 360 (2007) 272–281.
[11] A.C. Arokiam, A.V. Barasheva, D.J. Bacona, Yu.N. Osetsky, Philos. Mag. 85 (2005) 491–501.
[12] J. Cizek, F. Becvar, I. Prochazka, Nucl. Instrum. Meth. A 450 (2000) 325–337.
[13] M.J. Puska, R.M. Nieminen, Rev. Mod. Phys. 66 (1994) 841–897.
[14] R. Paulin, R. Ripon, Appl. Phys. 4 (1974) 343–347.
[15] J. Kansy, Nucl. Instrum. Meth. A 374 (1996) 235.
[16] A. Vehanen, P. Hautojarvi, J. Johansson, J. Yli-Kauppila, P. Moser, Phys. Rev. B 25 (1982) 762.
[17] G. Brauer, L. Liszkay, B. Molnar, R. Krause, Nucl. Eng. Des. 127 (1991) 47–68.
[18] T. Okita, N. Sekimura, F.A. Garner, L.R. Greenwood, W.G. Wolfer, Y. Isobe, Neutron-induced microstructural evolution of Fe–15Cr–16Ni Alloys at ~400 °C during neutron irradiation in the FFTF Fast Reactor. In: 10th International Conference on Environmental Degradation of Materials in Nuclear Power Systems – Water Reactors, 2001, issued on CD format.
[19] A.A. Chernobaeva et al., The Results of Reconstituted Specimens Testing of the VVER-440 Welds with Different Phosphorus Content after Irradiation, Annealing and Re-irradiation during 2 and 3 Campaigns in the Surveillance Channels of Rovno-1. Russian Research Center Kurchatov Institute, Report No. 180-16/10, Moscow, Russia, 2009.
[20] E.A. Kuleshova, B.A. Gurovich, Ya.I. Shtrombakh, Yu.A. Nikolaev, V.A. Pechenkin, J. Nucl. Mater. 342 (2005) 82.
[21] F. Bergner, A. Ulbricht, A. Gokhman, D. Erak, J. Nucl. Mater. 373 (2008) 199–205.
[22] V. Slugen, A. Zeman, J. Lipka, L. Debarberis, NDT&E Int. 37 (2004) 651–661.
[23] Ya.I. Shtrombakh, B.A. Gurovich, E.A. Kuleshova, D.Yu. Erak, S.V. Fedotova, D.A. Zhurko, O.O. Zabusov, Yu.A. Nikolaev, Atom. Energy 109 (2011) 257–265.